Scattering by a 2D Crack: The Meshfree Collocation Approach

B. Honarbakhsh[1] and A. Tavakoli[1, 2]

[1]Department of Electrical Engineering

[2]Institute of Communications Technology and Applied Electromagnetics
Amirkabir University of Technology (Tehran Polytechnic), Tehran, Iran
b_honarbakhsh@aut.ac.ir, tavakoli@aut.ac.ir

Abstract **─** In this paper, the meshfree collocation method is applied to the problem of EM scattering by a 2D crack in a PEC plane. The hybrid PDE-IE formulation is the mathematical statement of the problem. Consequently, the geometry and the filling material of the cavity is arbitrary. Validations are based on convergence analysis, modal solution and measurement results. Furthermore, elliminating numerical integrations has lead to a fast, accurate, and general meshfree solution.

Index Terms **─** Collocation, crack, FFT, mesh free, scattering.

I. INTRODUCTION

Electromagnetic (EM) scattering by a two-dimensional (2D) crack in a perfect electric conductor (PEC) plane is a well-known problem in computational electromagnetics (CEM). The problem is of high value in the fields of radar cross section (RCS) and non-destructive testing (NDT). This problem has two degrees of freedom; the shape of the gap and the gap filled material. When the shape and the gap material distribution are such that the computation of the modal Green's function of the gap is possible, the modal solution is preferable which leads to an integral equation (IE) and can be efficiently solved by the method of moments (MoM) [1]. For an arbitrary shaped but homogeneously filled gap, coupled system of IEs can formulate the problem and again, MoM can be used for numerical solution [2]. The most general case, i.e., an arbitrary shaped gap with arbitrary material distribution, can be well formulated by hybridizing a partial differential equation (PDE) governing the internal gap field (the interior problem) and the boundary integral (BI) governing the field over the PEC plane (the exterior problem), which has been handled by the hybrid FEM-BI method [3]. The problem is also studied by other approaches [4-6].

It is already reported that meshfree methods (MFMs) are more accurate than the FEM [7]. Furthermore, meshfree methods can solve the same problem by considerably fewer unknowns, leading to smaller size coefficient matrices and less memory usage. This advantage is due to the superb fitting capability of meshfree shape functions. Nevertheless, these methods are in general slower but not necessarily, compared to their mesh/grid based counterparts.

Being a weighted residual method, the kind of weighting function plays a key role in the computational cost of a meshfree method. Using the Dirac delta function as weighting leads to the meshfree collocation method which is the most computational efficient type. In comparison to plentiful research in the CEM community by numerical approaches such as FDTD, FEM and MoM, limited studies by meshless approaches are available in the literature such as [8-24].

In the present work, the aforementioned hybrid PDE-IE formulation is solved by the meshfree collocation method [25]. The IE part of the problem can potentially impair the speed of the solution by imposing numerical integration. Here, some suggestions are made to completely by-pass the integrations, leading to a general, accurate and fast meshfree solution for the problem.

Submitted On: Dec. 23, 2011
Accepted On: Feb. 9, 2012

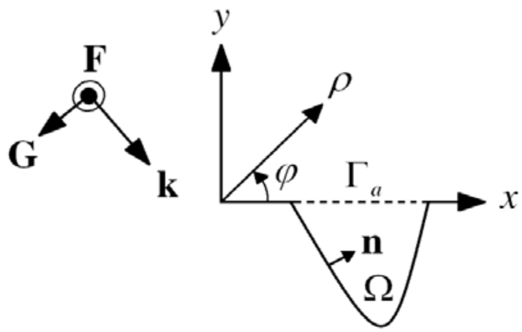

Fig. 1. Geometry description of the problem and definitions. Ω: crack domain, Γ_a: crack opening boundary, **F**/**G**: incident field, **k**: wave vector, **n**: normal vector to the crack wall.

II. MATHEMATICAL STATEMENTE OF THE PROBLEM

Geometry of the problem is depicted in Fig. 1. Based on the polarization of the incident wave, **F** and **G** are either of electric field vector **E** or magnetic field vector **H**. The wave number and intrinsic impedance of the free space are k_0 and Z_0, respectively. In addition, relative electric permittivity and magnetic permeability of the filling material are ε_r and μ_r, which are in general space dependent. Following [3], the mathematical statements of the problem for different incident polarizations are:

A. TE incidence

In this case, $\mathbf{F} = \mathbf{E} = \hat{\mathbf{z}}E$, $\mathbf{G} = \mathbf{H}$, and:

$$\begin{cases} \xi_{TE}(E) = 0, \ \rho \in \Omega \\ \mu_r^{-1} E_{,y}\big|_{y=0^-} + \gamma_{TE}\left(E\big|_{y=0^-}\right) = q_{TE}, \ \rho \in \Gamma_a \, . \\ E = 0, \ \rho \in \partial\Omega - \Gamma_a \end{cases} \tag{1}$$

where

$$\begin{cases} \xi_{TE}(\cdot) = \left(\mu_r^{-1}(\cdot)_{,x}\right)_{,x} + \left(\mu_r^{-1}(\cdot)_{,y}\right)_{,y} + k_0^2 \varepsilon_r(\cdot) \\ \gamma_{TE}(\cdot) = (j/2)\left(k_0^2 + _{,xx}\right) \int_{\Gamma_a} (\cdot) H_0^{(2)}\left(k_0 |x - x'|\right) dx' . \\ q_{TE}(x) = -j2k_0 Z_0 H_x^{inc}(x) \end{cases} \tag{2}$$

B. TM incidence

In this case, $\mathbf{F} = \mathbf{H} = \hat{\mathbf{z}}H$, $\mathbf{G} = \mathbf{E}$, and:

$$\begin{cases} \xi_{TM}(H) = 0, \ \rho \in \Omega \\ H\big|_{y=0^-} + \gamma_{TM}(H) = q_{TM}, \ \rho \in \Gamma_a \, . \\ H_{,n} = 0, \ \rho \in \partial\Omega - \Gamma_a \end{cases} \tag{3}$$

where:

$$\begin{cases} \xi_{TM}(\cdot) = \left(\varepsilon_r^{-1}(\cdot)_{,x}\right)_x + \left(\varepsilon_r^{-1}(\cdot)_{,y}\right)_y + k_0^2 \mu_r(\cdot) \\ \gamma_{TM}(\cdot) = (j2)^{-1} \int_{\Gamma_a} (\cdot)_{,y'}\big|_{y'=0^-} H_0^{(2)}\left(k_0 |x - x'|\right) dx' . \\ q_{TM}(x) = 2H_z^{inc}(x) \end{cases} \tag{4}$$

III. MESHFREE DISCRETIZATION

From a mathematical point of view, (1) and (4) are non-local boundary value problems and as stated before, can be decomposed into two parts: interior and exterior. The operator governing the interior problem is purely differential. Alternatively, the exterior operator is integro-differential. In view of intrinsic complexity of meshfree shape functions, improper selection leads to computational inefficiency. Radial interpolants and their partial derivatives are fast to generate with high order of continuity and excellent fitting ability [7, 25]. However, they work well when they are spread over the entire problem domain [26]. On the contrary, Shepard approximants while not as powerful, are still fast and localized on a small portion of the problem [27]. Therefore, we suggest expanding the field variable of the differential and integral parts of the problem over radial bases functions (RBFs) and Shepard functions, respectively.

Here, meshfree discretization of TE polarization is presented. The TM case can be carried out in a similar manner. Let the problem domain Ω and the whole boundary ∂Ω be described by N nodes with the first M nodes placed on Γ_a and the next $(N - P)$ nodes on the crack wall. Assume $\left\{\varphi_i^{(2D)}\right\}_{i=1}^{N}$, $\left\{\varphi_i^{(1D)}\right\}_{i=1}^{M}$ and $\left\{\psi_i^{(1D)}\right\}_{i=1}^{M}$ be sets of shape functions for corresponding nodes where superscripts represent the dimension of each set. In addition, mathematical functions u and v are defined for simplifying meshless discretization as:

$$\begin{cases} u(x) = (j/2)\int_{\Gamma_a} v(x') H_0^{(2)}\left(k_0 |x - x'|\right) dx' \\ v(x) = E(x, 0) \end{cases}. \quad (5)$$

Thus, $\gamma_{TE}\left(E|_{y=0^-}\right) = (j/2)\left(k_0^2 +_{,xx}\right)u(x)$. Following the aforementioned suggestion leads to expanding E and u over interpolants and v over approximants, e.g.:

$$\begin{cases} E^h(\rho) = \mathbf{\Phi}^{(2D)^T}(\rho)\cdot \hat{\mathbf{E}} = \sum_{i=1}^{N} \varphi_i^{(2D)}(\rho)\widehat{E_i} \\ u^h(x) = \mathbf{\Phi}^{(1D)^T}(x)\cdot \hat{\mathbf{u}} = \sum_{i=1}^{M} \varphi_i^{(1D)}(x)\widehat{u_i} \\ v^h(x) = \mathbf{\Psi}^{(1D)^T}(x)\cdot \hat{\mathbf{v}} = \sum_{i=1}^{M} \psi_i^{(1D)}(x)\widehat{v_i} \end{cases}, \quad (6)$$

with:

$$\begin{cases} \hat{\mathbf{E}} = \begin{bmatrix} \widehat{\mathbf{E}_G}^T & \widehat{\mathbf{E}_W}^T & \widehat{\mathbf{E}_C}^T \end{bmatrix} \\ \widehat{\mathbf{E}_G} = \begin{bmatrix} \widehat{E_1} \\ \vdots \\ \widehat{E_M} \end{bmatrix}, \widehat{\mathbf{E}_W} = \begin{bmatrix} \widehat{E_{M+1}} \\ \vdots \\ \widehat{E_P} \end{bmatrix}, \widehat{\mathbf{E}_C} = \begin{bmatrix} \widehat{E_{P+1}} \\ \vdots \\ \widehat{E_N} \end{bmatrix}, \\ \hat{\mathbf{u}} = \left[\widehat{u_1} \ldots \widehat{u_M}\right]^T, \hat{\mathbf{v}} = \left[\widehat{v_1} \ldots \widehat{v_M}\right]^T \end{cases} \quad (7)$$

where E^h and u^h are interpolated values of E and u, respectively, and v^h is the approximated value of v. Subscripts G, W and C denote gap, wall and internal crack nodes. For generating the system of equations, we collocate sides of (1) and (5) at the nodes. Considering the first equations in (1) and (6),

$$\xi_{TE}(E) = 0 \Rightarrow \sum_{q=1}^{N} \xi_{TE}\left[\varphi_q^{(2D)}(\rho_p)\right]\widehat{E_q} = 0, \quad \Rightarrow \mathbf{M}_1 \cdot \hat{\mathbf{E}} = 0. \quad (8)$$

where:

$$\left[\mathbf{M}_1\right]_{pq} = \xi_{TE}\left[\varphi_q^{(2D)}(\rho_p)\right]. \quad (9)$$

Next, substituting the expansion of u represented in (6) in the first equation of (5) leads to:

$$\sum_{q=1}^{M} \varphi_q^{(1D)}(\rho_p)\widehat{u_q} = \sum_{q=1}^{M}\left[(j/2)\int_{\Gamma_a} \psi_q^{(1D)}(x') H_0^{(2)}\left(k_0|\rho_p - x'|\right)dx'\right]\widehat{v_q}, \quad (10)$$

$$\Rightarrow \mathbf{M}_2 \cdot \hat{\mathbf{u}} = \mathbf{M}_3 \cdot \hat{\mathbf{v}}.$$

where:

$$\begin{cases} \left[\mathbf{M}_2\right]_{pq} = \varphi_q^{(1D)}(\rho_p) \\ \left[\mathbf{M}_3\right]_{pq} = (j/2)\int_{\Gamma_a} \psi_q^{(1D)}(x') H_0^{(2)}\left(k_0|\rho_p - x'|\right)dx' \end{cases}. \quad (11)$$

Similarly for v,

$$\sum_{q=1}^{M} \psi_q^{(1D)}(\rho_p)\widehat{v_q} = \sum_{q=1}^{N} \varphi_q^{(2D)}(\rho_p)\widehat{E_q},\ p \le M, \quad \Rightarrow \mathbf{M}_4 \cdot \hat{\mathbf{v}} = \mathbf{M}_5 \cdot \hat{\mathbf{E}}, \quad (12)$$

where:

$$\begin{cases} \left[\mathbf{M}_4\right]_{pq} = \psi_q^{(1D)}(x_p) \\ \left[\mathbf{M}_5\right]_{pq} = \varphi_q^{(2D)}(\rho_p),\ p \le M \end{cases}. \quad (13)$$

Finally, the second equation of (1) gives:

$$\sum_{q=1}^{N}\left[\mu_r^{-1}(\rho_p)\varphi_{q,y}^{(2D)}(\rho_p)\right]\widehat{E_q} + \sum_{q=1}^{M} j/2\left[k_0^2\varphi_q^{(1D)}(\rho_p) + \varphi_{q,xx}^{(1D)}(\rho_p)\right]\widehat{u_q} = q_{TE}, \quad (14)$$

$$\Rightarrow \mathbf{M}_6 \cdot \hat{\mathbf{E}} + \mathbf{M}_7 \hat{\mathbf{u}} = \hat{\mathbf{q}},$$

where:

$$\begin{cases} \left[\mathbf{M}_6\right]_{pq} = \mu_r^{-1}(\rho_p)\varphi_{q,y}^{(2D)}(\rho_p)\Big|_{y=0^-} \\ \mathbf{M}_7 = k_0^2\mathbf{M}_2 + \mathbf{M}_8 \\ \hat{\mathbf{q}} = \left[q_{TE}(x_1) \ \cdots \ q_{TE}(x_M)\right]^T \end{cases}, \quad (15)$$

with $\left[\mathbf{M}_8\right]_{pq} = (j/2)\varphi_{q,xx}^{(1D)}(x_p)$.

Therefore, the corresponding system of equation is:

$$\mathbf{M}_1 \cdot \hat{\mathbf{E}} = 0 \quad (16)$$

which can be uniquely solved after imposition of the following linear set of conditions:

$$\begin{cases} \left(\mathbf{M}_6 + \mathbf{M}_7\mathbf{M}_2^{-1}\mathbf{M}_3\mathbf{M}_4^{-1}\mathbf{M}_5\right)\hat{\mathbf{E}} = \hat{\mathbf{q}} \\ \widehat{\mathbf{E}_W} = 0 \end{cases} \quad (17)$$

Once $\hat{\mathbf{E}}$ is computed, the field variable E can be interpolated at any point in the domain and on the problem boundary.

IV. COMPUTING THE ENTRIES OF $\mathbf{M}_3$

Among $\mathbf{M}_i$ matrices, $1 \le i \le 8$, The only time-consuming one is $\mathbf{M}_3$. In this section, two approaches are suggested for this purpose, one in the space domain and the other in the spectral domain. The latter is our proposed method.

A. Space domain

A choice of computing the entries of $\mathbf{M}_3$ in the space domain is performing the following two steps. First, the Green's function is decomposed into singular and oscillatory parts, i.e.:

$$G = G_{Sing} + G_{Oscill}, \tag{18}$$

where:

$$\begin{cases} G = H_0^{(2)}(k_0\rho) \\ G_{Sing} = (2/j\pi)\ln(k_0\rho) \\ G_{Oscill} = H_0^{(2)}(k_0\rho) - (2/j\pi)\ln(k_0\rho) \end{cases}. \tag{19}$$

Second, the oscillatory part is integrated by a standard quadrature, e.g. Gauss-Legendre and the singular part by the quadrature rule given in [28].

B. Spectral domain

This is our suggested method and requires the crack nodes to be arranged equidistance. By doing so, all of the $\psi_i^{(1D)}$ shape functions are shifted version of each other. Furthermore, the study of Shepard functions shows that they can be well approximated by a single Gaussian function. Thus, the mathematical form of the $\mathbf{M}_3$ entries can be approximated by:

$$\begin{cases} P = S * G \\ S(\rho) = \alpha \exp(-\beta\rho^2) \end{cases}, \tag{20}$$

where α and β are positive real constants to be determined by approximating a representative such as the central node approximant by a Gaussian function. Here, "*" stands for linear convolution. Since the spectrum of a Gaussian function is practically band limited, (18) could be efficiently computed by the fast Fourier transform (FFT), i.e.:

$$P = FFT^{-1}\{FFT\{S\}\cdot FFT\{G\}\}. \tag{19}$$

V. NUMERICAL RESUILTS

In this section, we have applied the proposed meshfree method to the same problems addressed in [3], with the geometry as depicted in Fig. 2. The convergence analysis curves are provided for rigorously validating the method [29]. Thin-plate spline (TPS) functions are used for construction of meshfree shape functions [7]. The influence domain of Shepard functions are selected to be $1.5\times(D_x^2 + D_y^2)^{1/2}$ where D_x and D_y are nodal spacing in x and y directions, respectively. Additionally, for error estimate we used:

$$r_e(u_1, u_2) = \|u_1 - u_2\| / \|u_1\|, \tag{20}$$

where $\|u\| = 1/2\left(\int_\Omega |u|^2\, d\Omega\right)^{1/2}$.

Consider a gap with w = 1λ and d = 0.25λ. Two sets of supporting nodes are used for meshless discretization; regular and randomly distributed, as depicted in Fig. 3. Figure 4 depicts the convergence curves for both polarizations and different filling materials at normal incidence based on regular node arrangement. The electric filed distribution at the crack opening for normal TE incidence for both node arrangements are depicted in Fig. 5 and the modal solution that validates the proposed method. Normalized scattering width as a function of incidence angle and frequency for TE and TM polarizations are depicted in Fig. 6, assuming regular node arrangement. Finally, the computational cost of evaluating $\mathbf{M}_3$ entries in space and spectral domains are compared in Fig. 7.

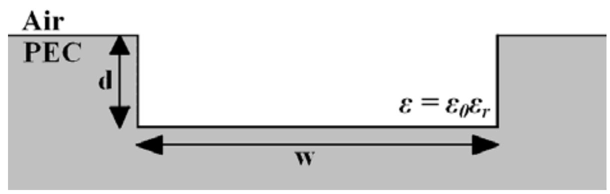

Fig. 2. Geometry of the rectangular crack.

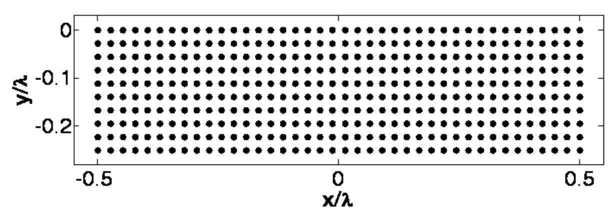

(a)

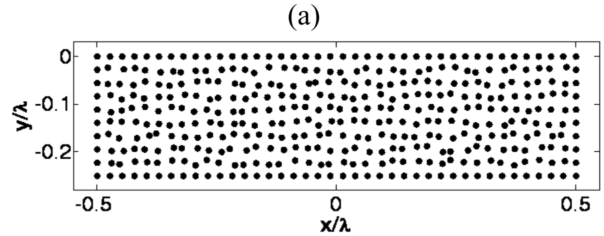

(b)

Fig. 3. Node arrangements in the rectangular crack with w = 1λ, d = 0.25λ: (a) regular, (b) random.

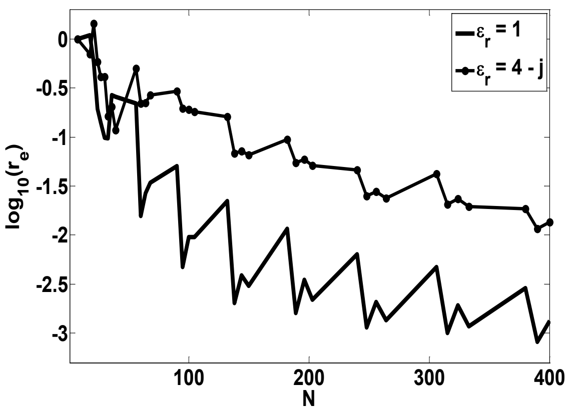

(a)

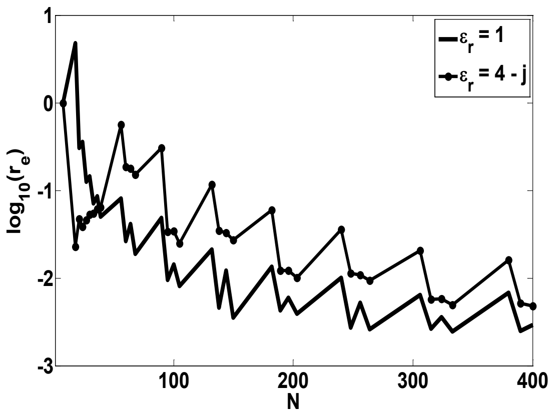

(b)

Fig. 4. Convergence curves for w = 1λ and d = 0.25λ at normal incidence: (a) TE polarization. (b) TM polarization.

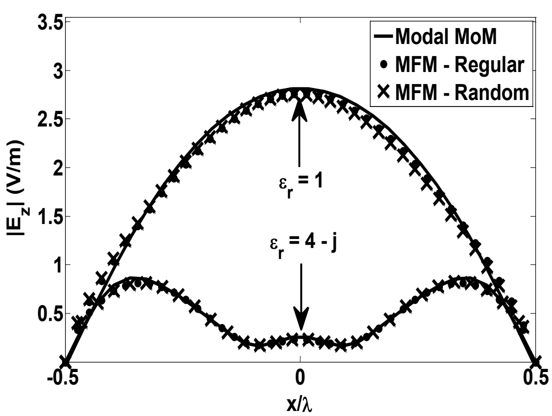

(a)

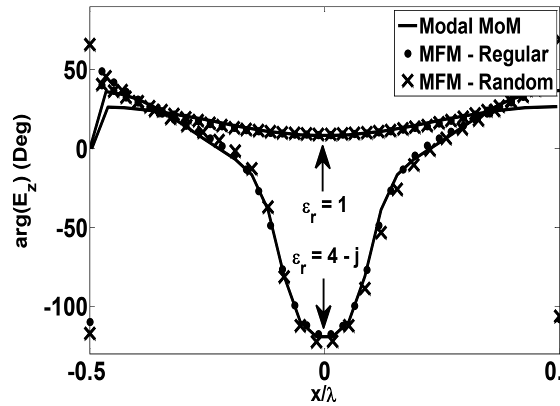

(b)

Fig. 5. Electric filed distribution at the crack opening for w = 1λ and d = 0.25λ at normal TE incidence: (a) magnitude, (b) phase.

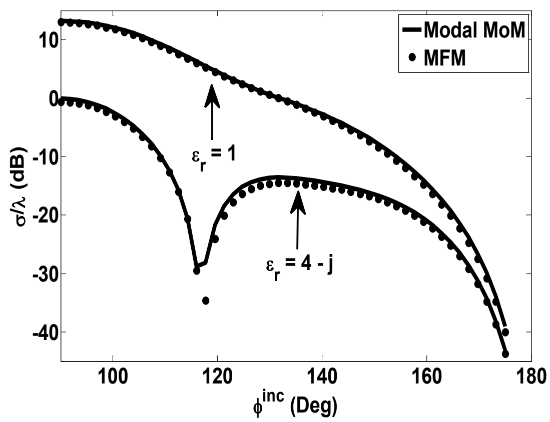

(a)

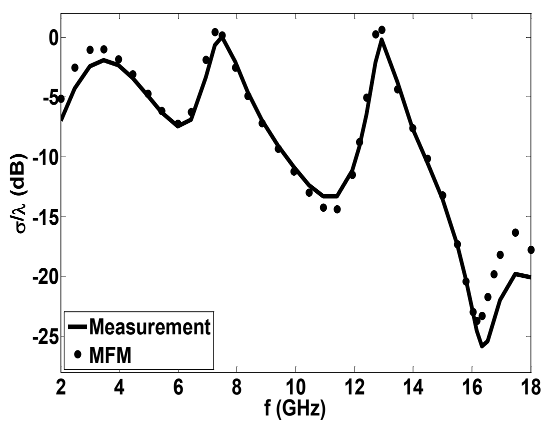

(b)

Fig. 6. Normalized scattering width as a function of (a) angle for w = 1λ and d = 0.25λ for TE incidence, (b) frequency for w = 2.5 cm and d = 1.25 cm for an air filled crack for TM incidence at φ = 10° (measurement results from [3]).

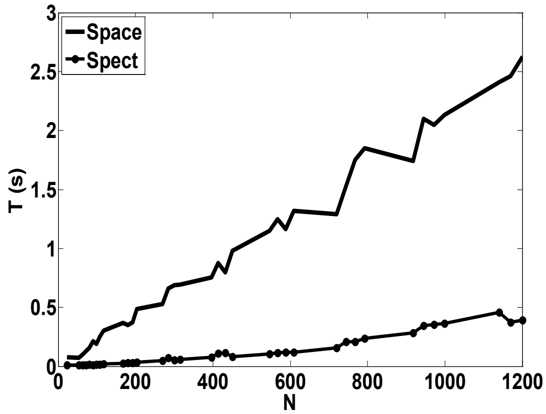

Fig. 7. Computational cost of evaluating $\mathbf{M}_3$ entries in space and spectral domains for a sample simulation.

VI. CONCLUSION

In this paper, the problem of EM scattering by a 2D crack is solved by meshfree collocation method. The selected formulation is hybrid PDE-IE that can handle a general shaped crack filled with an arbitrary material. A proper choice of meshless shape functions for PDE and IE parts are used for efficient meshless discretization. Additionally, a method is proposed to bypass numerical integration by exploiting FFT. Thus, a general, fast, and accurate meshfree method is developed. Convergence analysis, modal solution, and measurement data validate the approach.

ACKNOWLEDGMENT

The authors appreciate Prof. M. Dehghan for inputs in meshfree methods.

REFERENCES

[1] K. Barkeshli, J. L. Volakis, “Scattering by a Two Dimensional Groove in a Ground Plane,” Technical report for NASA grant NAG-2-541, The Radiation Laboratory, Department of Electrical Engineering and Computer Science, The University of Michigan, Ann Arbor, MI, 1989.

[2] T. B. A. Senior, K. Sarabandi, and J. R. Natzke, “Scattering by Narrow Gap,” *IEEE Trans. Antennas Propagat.*, vol. 38, no. 7, pp. 1102-1110, 1990.

[3] J. Jin, *The Finite Element Method in Electromagnetics, Second Edition*. John Wiley & Sons, 2002.

[4] M. Bozorgi and A. Tavakoli, “Polarimetric Scattering from a 3-D Rectangular Crack in a PEC Covered by a Dielectric Layer,” *Applied Computational Electromagnetics Society (ACES) Journal*, vol. 26, no. 6, pp. 502 - 511, June 2011.

[5] F. Deek, M. El-Shenawee, “Microwave Detection of Cracks in Buried Pipes using the Complex frequency Technique,” *Applied Computational Electromagnetics Society (ACES) Journal*, vol. 25, no. 10, pp. 894 - 902, October 2010.

[6] Richard K. Gordon, W. Elliott Hutchcraft, “The Use of Multiquadric Radial Basis Functions in Open Region Problems,” *Applied Computational Electromagnetics Society (ACES) Journal*, vol. 21, no. 2, pp. 127 - 134, July 2006.

[7] G. R. Liu, *Mesh Free Methods*. CRC Press, 2003.

[8] Y. Marechal, “Some Meshless Methods for Electromagnetic Field Computations,” *IEEE Trans. Magn.*, vol. 34, no. 5, pp. 3351-3354, 1998.

[9] C. Herault and Y. Marechal, “Boundary and Interface Conditions in Meshless Methods,” *IEEE Trans. Magn.*, vol. 35, no. 3, pp. 1450-1453, 1999.

[10] S. L. Ho, S. Yang, J. M. Machado, and H. C. Wong, “Application of a Meshless Method in Electromagnetics,” *IEEE Trans. Magn.*, vol. 37, no. 5, pp. 3198-3201, 2001.

[11] L. Xuan, Z. Zeng, B. Shanker, and L. Udpa, “Meshless Method for Numerical Modeling of Pulsed Eddy Currents,” *IEEE Trans. Magn.*, vol. 40, no. 6, pp. 3457-3462, 2004.

[12] S. L. Ho, S. Shiyou Yang, H. C. Wong, and G. Ni, “Meshless Collocation Method Based on Radial Basis Functions and Wavelets,” *IEEE Trans. Magn.*, vol. 40, no. 2, pp. 1021-1024, 2004.

[13] S. L. Ho, S. Shiyou Yang, G. Ni , H. C. Wong, and Y. Wang, “Numerical Analysis of Thin Skin Depths of 3-D Eddy-Current Problems using a Combination of Finite Element and Meshless Methods,” *IEEE Trans. Magn.*, vol. 40, no. 2, pp. 1354-1357, 2004.

[14] S. L. Ho, S. Shiyou Yang, H. C. Wong, E. W. C. Lo, and G. Ni, “Refinement Computations of Electromagnetic Fields using FE and Meshless Methods,” *IEEE Trans. Magn.*, vol. 41, no. 5, pp. 1456-1459, 2005.

[15] Y. Zhang, K. R. Shao, D. X. Xie, and J. D. Lavers, “Meshless Method Based on Orthogonal Basis for Electromagnetics,” *IEEE Trans. Magn.*, vol. 41, no. 5, pp. 1432-1435, 2005.

[16] Q. Li and K. Lee, “Adaptive Meshless Method for Magnetic Field Computation,” *IEEE Trans. Magn.*, vol. 42, no. 8, pp. 1996-2003, 2006.

[17] Y. Zhang, K. R. Shao, J. Zhu, D. X. Xie, and J. D. Lavers, “A Comparison of Point Interpolative Boundary Meshless Method Based on PBF and RBF for Transient Eddy-Current Analysis,” *IEEE Trans. Magn.*, vol. 43, no. 4, pp. 1497-1500, 2007.

[18] F. G. Guimaraes, R. R. Saldanha, R. C. Mesquita, D. A. Lowther, and J. A. Ramirez, “A Meshless

Method for Electromagnetic Field Computation Based on the Multiquadratic Technique," *IEEE Trans. Magn.*, vol. 43, no. 4, pp. 1281-1284, 2007.

[19] S. Ikuno, K. Takakura, and A. Kamitani, "Influence of Method for Imposing Essential Boundary Condition on Meshless Galerkin/Petrov-Galerkin Approaches," *IEEE Trans. Magn.*, vol. 43, no. 4, pp. 1501-1504, 2007.

[20] S. McFee, D. Ma, and M. Golshayan, "A Parallel Meshless Formulation for *h-p* Adaptive Finite Element Analysis," *IEEE Trans. Magn.*, vol. 44, no. 6, pp. 786-789, 2008.

[21] Y. Yu and Z. Chen, "Towards the Development of an Unconditionally Stable Time-Domain Meshless Method," *IEEE Trans. Microwave Theory Tech*., vol. 58, no. 3, pp. 578- 586, 2010.

[22] Y. Yu and Z. Chen, "A 3-D Radial Point Interpolation Method for Meshless Time-Domain Modeling," *IEEE Trans. Microwave Theory Tech.*, vol. 57, no. 8, pp.2015-202, 2009.

[23] T. Kaufmann, C. Fumeaux, and R. Vahldieck, "The Meshless Radial Point Interpolation Method for Time-Domain Electromagnetics," *IEEE MTT-S Int. Microwave Symp. Dig.*, Atlanta, pp. 61 - 64, 2008.

[24] T. Kaufmann, C. Engströ̈m, C. Fumeaux, and R. Vahldieck, "Eigenvalue Analysis and Longtime Stability of Resonant Structures for the Meshless Radial Point Interpolation Method in Time Domain," *IEEE Trans. Microwave Theory Tech*, vol. 58, pp. 3399 - 3408, 2010.

[25] G. R. Liu and Y. T. Gu, *An Introduction to MeshFree Methods and Their Programming*. Springer, 2005.

[26] R. Schaback, "Limit problems for interpolation by analytic radial base functions," *Comp. Appl. Math.*, vol. 212, no. 2, pp. 127-149, 2008.

[27] D. Shepard, "A Two Dimensional Interpolation Function for Irregularly Spaced Data," in *Proc. 23rd Nat. Conf. ACM*, 1968, pp. 517–523.

[28] A. H. Stroud and D. Secrest, *Gaussian Quadrature Formulas*, Prentice Hall, N.Y., 1966.

[29] J. C. Rautio, "The Microwava Point of View on Software Validation," *IEEE Antennas Propagat. Mag*., vol. 38, no. 2, pp. 68-71, 1996.

Babak Honarbakhsh was born in Tehran, Iran. He received his B.S. and M.S. degrees in Electrical Engineering from Amirkabir University of Technology where he is currently working toward his Ph.D. degree. His current research interest is numerical solution of electromagnetic problems by mesh free methods.

Ahad Tavakoli was born in Tehran, Iran, on March 8, 1959. He received B.S. and M.S. degrees from the University of Kansas, Lawrence, and the Ph.D. degree from the University of Michigan, Ann Arbor, all in Electrical Engineering, in 1982, 1984, and 1991, respectively.

He is currently a Professor in the Department of Electrical Engineering at Amirkabir University of Technology. His research interests include EMC, scattering of electromagnetic waves and microstrip antennas.